Metabolic Engineering Communications 13 (2021) e00173

Contents lists available at ScienceDirect

Metabolic Engineering Communications

journal homepage: www.elsevier.com/locate/mec

Engineering *Acinetobacter baylyi* ADP1 for mevalonate production from lignin-derived aromatic compounds

Erika Arvay [a,b], Bradley W. Biggs [a,b], Laura Guerrero [c], Virginia Jiang [d], Keith Tyo [a,*]

[a] Department of Chemical and Biological Engineering, Northwestern University, Evanston, IL, USA
[b] Biotechnology Training Program, Northwestern University, Evanston, IL, USA
[c] Department of Biomedical Engineering, University of Wisconsin-Madison, Madison, WI, USA
[d] Department of Chemical Engineering, Columbia University, New York, NY, USA

ARTICLE INFO

Keywords:
Acinetobacter baylyi ADP1
Lignin
Mevalonate
Metabolic engineering
Renewable chemistry

ABSTRACT

Utilization of lignin, an abundant renewable resource, is limited by its heterogenous composition and complex structure. Biological valorization of lignin provides advantages over traditional chemical processing as it occurs at ambient temperature and pressure and does not use harsh chemicals. Furthermore, the ability to biologically funnel heterogenous substrates to products eliminates the need for costly downstream processing and separation of feedstocks. However, lack of relevant metabolic networks and low tolerance to degradation products of lignin limits the application of traditional engineered model organisms. To circumvent this obstacle, we employed *Acinetobacter baylyi* ADP1, which natively catabolizes lignin-derived aromatic substrates through the β-ketoadipate pathway, to produce mevalonate from lignin-derived compounds. We enabled expression of the mevalonate pathway in ADP1 and validated activity in the presence of multiple lignin-derived aromatic substrates. Furthermore, by knocking out wax ester synthesis and utilizing fed-batch cultivation, we improved mevalonate titers 7.5-fold to 1014 mg/L (6.8 mM). This work establishes a foundation and provides groundwork for future efforts to engineer improved production of mevalonate and derivatives from lignin-derived aromatics using ADP1.

1. Introduction

Lignin is the second most abundant biomass-derived carbon source on Earth and represents a renewable reservoir of energy-dense substrate to perform green chemistry (Ragauskas et al., 2014). Annual worldwide production is approximately fifty-million tons, and this production is projected to increase significantly as it is a byproduct of biofuel production technology (Norgren and Edlund, 2014). Due to the variability in both composition and bonding structure of lignin, processing is challenging (Linger et al., 2014; Schutyser et al., 2018). Furthermore, utilization of processed lignin is difficult due to the inherent compositional heterogeneity of lignin degradation products. Currently, most lignin is treated either as a waste stream or is burned as a solid fuel in biorefinement processes (Schutyser et al., 2018). However, biological upgrading, or valorization of lignin provides advantages over traditional chemical processing or combustion by enabling conversion of diverse lignin-derived substrates to high value products (Linger et al., 2014).

Aromatics-degrading microorganisms can catabolize the broad range of substrates found in processed lignin (Salvachúa et al., 2015). The substrate funneling characteristic of microbial lignin-derived aromatics metabolism allows for the utilization of diverse lignin-derived compounds without prior separation. Several microorganisms, including *Rhodococcus* and *Pseudomonas* species, can synthesize a range of products like triacylglycerols (TAGs) and polyhydroxyalkanoate (PHA) from lignin derivatives (Linger et al., 2014; MacEachran and Sinskey, 2013). *Acinetobacter baylyi* ADP1 represents a promising candidate for biological valorization of lignin-derived compounds (Beckham et al., 2016). In addition to its versatile metabolism, it possesses natural competence and native homologous recombination machinery that enable rapid and targeted genomic manipulations (Barbe et al., 2004; Elliott and Neidle, 2011). Emerging tools for ADP1 have further broadened the feasible scope of engineering and enabled rapid iteration through design-build-test-learn cycles (Biggs et al., 2020; Suárez et al., 2019).

Leveraging the advantageous characteristics of ADP1, we engineered a strain capable of expressing the mevalonate pathway during growth on lignin-related aromatic substrates. Mevalonate is a small molecule with

* Corresponding author.
E-mail address: k-tyo@northwestern.edu (K. Tyo).

https://doi.org/10.1016/j.mec.2021.e00173
Received 15 May 2020; Received in revised form 4 May 2021; Accepted 5 May 2021
Available online 24 May 2021

applications in cosmetics and as a monomer precursor to some classes of polyesters (Wang, 2017). It is also a precursor to terpenoids that have applications in industries ranging from biofuels production to flavorings and fragrances (Ajikumar et al., 2008; Belcher et al., 2020; Zhang et al., 2017). The dedicated pathway for mevalonate synthesis requires three acetyl-CoA and two NADPH molecules, which at high flux can strain native metabolism. Thus, expression of this pathway in ADP1 provides an opportunity to study the impact of acetyl-CoA and NADPH siphoning in ADP1 as well as to identify potential obstacles to be overcome towards utilization of ADP1 as a production host. We show mevalonate pathway activity in the presence of various lignin-derived aromatic compounds and improved productivity by eliminating the resource competitive wax ester pathway. In addition, we conducted fed-batch cultures to evaluate productivity over time. This work demonstrates ADP1 as a host for biological valorization of lignin-derived substrates to mevalonate and adds to the body of previous efforts (Ishige et al., 2002; Luo et al., 2019; Santala et al., 2011, 2014) to synthesize industrially important products using ADP1's potential as an metabolic engineering host and indicates targets for future engineering.

2. Materials and methods

2.1. Strains and media

In this study wild type (WT) ADP1 was obtained from the Ellen Neidle lab (U. Georgia) and used for cloning (Juni and Janik, 1969; Vaneechoutte et al., 2006). The mevalonate plasmid was constructed using pBWB162 (Addgene #140634) (Biggs et al., 2020) vector and pJBEI-6410 (Addgene #47049) (Alonso-Gutierrez et al., 2013) mevalonate pathway. The plasmid pBWB290 was used to perform genomic knock-out via SacB/Kan^R. Genomic DNA used to amplify genome homology for the genomic knock-out was isolated using a Wizard Genomic DNA Purification kit (Promega).

Initial precultures for mevalonate production were grown in LB Broth (Fisher Scientific). M9 minimal medium (1L) was prepared in sterile filtered water with 2 mM $MgSO_4$ (heptahydrate, Sigma Aldrich), 0.1 mM $CaCl_2$ (dihydrate, Sigma Aldrich), 0.18% (w/v) (10 mM) glucose solution (unless otherwise noted) (monohydrate, Acros Organics), and M9 Minimal Salts (BD Difco) (239 μM disodium phosphate, 110 μM monopotassium phosphate, 43 μM sodium chloride, 93 μM ammonium chloride). Aromatic carbon sources were supplied at 20 mM, 10 mM, 5 mM, or 2 mM as noted from 0.5M protocatechuate (PCA) (pH 7, adjusted with 10N NaOH) (Sigma Aldrich), 0.5M *p*-hydroxybenzoate (POB) (pH 7, adjusted with 10 N NaOH) (Sigma Aldrich), 0.25 M ferulate (pH 7, adjusted with 10 N NaOH) (Sigma Aldrich), 0.5 M benzoate (pH 7, adjusted with 10 N sodium hydroxide) (Sigma Aldrich), or 0.5 M anthranilate (pH 7, adjusted with 10 N NaOH) (Sigma Aldrich). Kanamycin was used at a working concentration of 25 mg/L for ADP1 cultures requiring antibiotic for plasmid maintenance.

2.2.1. General cloning

Plasmids were purified using a GeneJet Plasmid Miniprep kit (Thermo Scientific). All PCRs were performed with DNA oligomer primers (10 μM) (IDT DNA) and 2X PrimeSTAR Max DNA polymerase (Takura Bio). PCR products were purified from agarose gel using a GeneJet Gel Extraction kit (Thermo Scientific). Plasmid assembly was performed via Gibson assembly using 2X Gibson Assembly Master Mix (NEB) (Gibson et al., 2009).

2.2.2. Construction of plasmids

The mevalonate pathway was cloned into pBWB162, which is derived from the broad host range vector pBAV1k and is capable of *E. coli* and ADP1 replication (Bryksin and Matsumura, 2010). The upper mevalonate pathway (AtoB, ERG1, and HMG1) was amplified from the pJBEI-6410 (Addgene #47049) (Alonso-Gutierrez et al., 2013) plasmid using primers ECA01/02 (Supplemental Table 1). The vector backbone containing an ADP1-compatible origin, kanamycin resistance marker, *lacI*, *lacO*, and the IPTG-inducible p_{trc} promoter region was amplified from pBWB162 (Addgene #140634) (Biggs et al., 2020) using primers ECA03/04. Gibson assembly was used to piece together the mevalonate pathway insert with the pBWB162 backbone to create pMev-LacI-trc (pECA03). This plasmid was sequenced then transformed into WT ADP1, as previously described (Biggs et al., 2020) to generate strain ADP1 pMev-LacI-trc (ECA10).

To enable strong expression of levansucrase, *sacB* was placed under control of the p_{trc} promoter on the pBWB162 vector. The vector pBWB162 was amplified using primers BWB645/646, and *sacB* was amplified using primers BWB647/648. The gel-extracted DNA fragments were assembled using Gibson assembly to generate pBWB290.

2.2.3. Construction of acr1 knock-out strains ADP1 Δacr1 (ECA14) and ADP1 Δacr1 pMev-LacI-trc (ECA15)

This knock-out was performed using SacB/Kan^R counterselection adapted from Metzgar et al. (2004). Genome homology of 500 bp flanking *acr1* was amplified from ADP1 genomic DNA using primers ECA05/06 (forward homology) and ECA09/10 (back homology). The SacB/Kan^R cassette, containing SacB downstream of the p_{trc} promoter and Kan^R, was amplified from pBWB290 using primers ECA07/08. The parts were assembled into the trc-SacB/KanR selection cassette using overlap extension PCR (Anton V. Bryksin and Ichiro Matsumura, 2010) with primers ECA05/10. The trc-SacB/KanR selection cassette was gel extracted and transformed into WT ADP1 to create ADP1Δ*acr1*::trc-SacB/Kan^R. Transformants were plated on kanamycin LB agar plates and incubated at 30 °C overnight. The next day, 32 transformant colonies were patched onto kanamycin LB agar plates and sucrose LB agar plates to confirm sucrose sensitivity. These plates were incubated at ambient (~22 °C) temperature for 24–48 hours (Blomfield et al., 1991), and colonies that displayed kanamycin resistance and sucrose sensitivity were selected from the kanamycin LB agar plate. These colonies were clonally purified by streaking again on kanamycin LB agar and on sucrose LB agar and growing for 24–48 hours at ambient temperature. Clonally pure colonies were validated for integration of the SacB/Kan cassette at the *acr1* locus using colony PCR and primers ECA15/16.

To delete trc-SacB/Kan^R from the ADP1 genome, a counterselection cassette was constructed. First, the forward and back homologies flanking *acr1* on the ADP1 genome were amplified from the ADP1 genome using primers ECA11/12 (forward homology) and ECA13/14 (back homology). Then the *acr1* counterselection cassette comprising the forward and back homologies was created using overlap extension PCR with primers ECA11/14. ADP1 Δ*acr1*::trc-SacB/Kan^R was transformed with the *acr1* counterselection cassette, and transformants were incubated for 24–48 hours at ambient temperature. Subsequent colonies were screened for loss of the SacB/Kan^R cassette by patching onto sucrose LB agar and kanamycin LB agar plates and incubating for 24–48 hours at ambient temperature. Colonies that displayed no growth inhibition on sucrose LB agar and did not grow on kanamycin LB agar were clonally purified by patching onto kanamycin LB agar and sucrose LB agar again and incubating overnight at ambient temperature. Colonies that grew only on sucrose LB agar were screened for loss of the original *acr1* gene via colony PCR with primers ECA15/16. Colonies with apparent deletion were sequence validated to generate ADP1 Δ*acr1* (ECA14). pMev-LacI-trc (pECA03) was transformed into ADP1 Δ*acr1* (ECA14) to generate ADP1 Δ*acr1* pMev-LacI-trc (ECA15).

2.3. Culture conditions

2.3.1. General culture conditions

All ADP1 mevalonate production cultures were grown at 30 °C and 250 rpm with 25 mg/L kanamycin for plasmid maintenance in 125 mL unbaffled Erlenmeyer flasks unless otherwise noted. Precultures were started by inoculating 5 mL LB medium from glycerol stocks and grown for 12–16 hours. Cells were then transferred to 25 mL M9 minimal

medium supplemented with aromatic acids and glucose as carbon sources and grown for an additional 12–16 hours prior to inoculation into cultures. To inoculate M9 minimal medium cultures, a sample of preculture was centrifuged at 4000×*g* and 4 °C for 10 minutes. Spent supernatant was removed, cell pellets were resuspended in M9 minimal medium to an optical density of 5 and inoculated into 25 mL M9 minimal medium at a 1:100 dilution. Following growth to OD 0.6, the expression of the mevalonate pathway was induced with 1 mM IPTG.

2.3.2. Varied aromatic growth rate culture conditions

For growth rate measurements of ADP1 in varied aromatic media, optical density was measured using a Synergy H1 microplate reader (BioTek) and Flat Bottom Clear Non-sterile 96-well plates (Fisherbrand). Precultures were grown initially in 5 mL LB overnight, then diluted 1:100 into 5 mL of M9 minimal medium containing 10 mM (0.18% w/v) glucose and either POB, ferulate, benzoate, or anthranilate at either 20 mM or 5 mM and allowed to grow for an additional 16 hours in 5 mL precultures. Precultures were then spun down to pellet cells and resuspended at an OD of 0.05 in fresh medium and pipetted into wells. Each well contained 300 μL of culture. Blank wells containing sterile media were placed alongside culture wells to control for contamination as well as measure blank absorbance. Unmeasured wells were filled with water to minimize evaporation. The plate reader was held at 30 °C and 250 rpm shaking for 14 hours with absorbance readings every 15 minutes.

2.3.3. Fed-batch culture conditions

All fed-batch cultures were precultured in LB then M9 medium and inoculated at an OD of 0.05 as described above. All strains and conditions started with M9 minimal medium initially containing 20 mM POB and 10 mM glucose. After 24 hours of growth, 20 mM POB was added to the POB-fed culture, 20 mM glucose was added to the glucose-fed culture, and sterile water was added to the non-fed culture to control for dilution. An equal volume was added to each culture to prevent dilution affects from influencing observed trends. Every 24 hours cultures were sampled and analyzed for mevalonate concentration and substrate concentration before and after carbon addition. After 168 hours of growth, final samples were collected, and cell pellets were analyzed for truncation of the mevalonate pathway via colony PCR.

2.4. Analytical methods

2.4.1. Sampling

For fed-batch cultures, optical density readings were taken every 24 hours. All optical density readings were taken using a Synergy H1 microplate reader (BioTek) and Flat Bottom Clear Non-sterile 96-well plates (Fisherbrand). 300 μL of total volume was pipetted into each well with appropriate dilution by fresh M9 medium.

Prior to addition of the desired carbon source to fed-batch cultures, 250 μL samples were collected. These samples were centrifuged immediately at maximum speed (17,000×*g*) and 4 °C for 10 minutes. Culture supernatant was transferred to clean tubes and stored at 4 °C until analysis by HPLC or GC-MS (below). The mevalonate pathway cassette from the final timepoint cell pellet was amplified by colony PCR (cPCR) using primers ECA17/18 to screen for large pathway deletions. The cPCR amplified mevalonate pathway DNA was purified via gel extraction and sequenced to identify mutations.

2.4.2. High pressure liquid chromatography (HPLC) sample analysis

After centrifugation, 80 μL of supernatant sample was pipetted into 250 μL polyspring glass inserts placed into glass screw top vials then sealed with PTFE/silicone caps (Filtrous). Samples were analyzed using an Agilent 1200 Series HPLC equipped with a BioRad HPX-87H chromatography column, an Agilent G1315C Diode Array Detector (DAD), and an Agilent G1362A Refractive Index Detector (RID). The mobile phase was 10% (v/v) acetonitrile, 90% (v/v) 5 mM sulfuric acid (Thermo). The column was equilibrated for 1 hour at a flow rate of 0.600 mL/min and a column temperature of 60 °C. Following equilibration at 0.600 mL/min at 60 °C, the following method was used to run samples. The injection volume was 5.00 μL. Run time was 30 minutes with post-time of 1 minute. The autosampler was maintained at a temperature of 4 °C and the RID at a temperature of 35 °C. The DAD signal at 194 nm was used to quantify aromatic acids and gluconate, and the RID signal was used to quantify glucose. Standards were run for each aromatic acid, for gluconate, (Sigma-Aldrich) and for glucose to determine retention times and to generate standard curves.

2.4.3. Gas chromatography Mass spectrometry (GCMS) sample analysis

Samples were extracted into ethyl acetate for GCMS analysis using a method adapted from previous work (Dueber et al., 2009). For each extraction, 20 μL of culture supernatant was placed into a 1.2 mL Eppendorf tube. To this, an extraction standard of 2 μL of 10 g/L β-carophyllene in ethyl acetate was added. To catalyze the lactonization of mevalonate to mevalonolactone, 10 μL of 0.5 N hydrochloric acid was added. The sample was vortexed briefly prior to the addition of 190 μL of ethyl acetate. The sample was then sealed and shaken at 1400 rpm for 5 minutes, then centrifuged at maximum speed (17,000×*g*) at 4 °C for 5 minutes. The organic (lower density) fraction was pipetted into a 250 μL glass polyspring insert in a glass screw top vial and then sealed with a PTFE/silicone cap (Filtrous). Samples were analyzed immediately after extraction. The following method was used to analyze samples using an Agilent 7890 GC equipped with an Agilent HP-5ms Ultra Inert column (30 m x 250 μm x 0.25 μm) and an Agilent 7000 MS. The injection volume was 1 μL. Helium was used as the carrier gas. The front inlet was run on splitless mode at a temperature of 150 °C and a pressure of 12.5 psi with a total flow rate of 54 mL/min and a septum purge flow of 3 mL/min. The MSD transfer line was held at 290 °C. The oven was set to an initial temperature of 60 °C with a ramp rate of 15 °C/min to 200 °C with a hold time of 1 minute. Post-run was held at 300 °C for 5 minutes.

Standards of 100 mg/L β-caryophyllene were run alongside samples to normalize for extraction. 0.13% (w/v) (10 mM) mevalonolactone standards in ethyl acetate were also run alongside samples. Mevalonolactone concentration was calculated from a standard curve of mevalonolactone in ethyl acetate. Yields were calculated from the mevalonate titer and substrate consumption as calculated from initial and final substrate concentrations. Carbon yields were calculated based upon the carbon atoms present in mevalonate and the respective substrates. For mixed substrate cultivations, c-mmol/c-mol yields were calculated based on the carbon yield for the combined substrates.

3. Results and discussion

3.1. Mevalonate pathway is functionally expressed in ADP1, but not genetically stable in protocatechuate-only medium

Initial validation of pathway functionality was performed by culturing ADP1 pMev-LacI-trc (ECA10) in minimal M9 medium under three conditions. One condition was supplied with 1.54 g/L (10 mM) PCA, a metabolic intermediate in the catabolism of lignin-derived aromatic compounds, as the sole carbon source. A second condition was supplied with 0.31 g/L (2 mM) PCA and 0.2% (w/v) (11.1 mM) glucose. The last condition was supplied with 1.54 g/L (10 mM) PCA and 0.2% (w/v) (11.1 mM) glucose. Mevalonate and cell density was measured after 24 hours of cultivation in all conditions [Fig. 1 B]. These data indicate that the mevalonate pathway can be expressed functionally in ADP1, and based on the PCA-only condition, can produce mevalonate solely from an aromatic, lignin-related carbon source ($p < 0.01$ relative to no mevalonate control). Notably, cultures containing PCA as the sole carbon source accumulated very little mevalonate and grew to a lower OD in comparison to cultures supplemented with glucose (Fig. 1 B). pMev-LacI-trc (pECA03) plasmids were isolated at 24 hours and sequenced for each culture. Sequencing revealed partial deletions of the

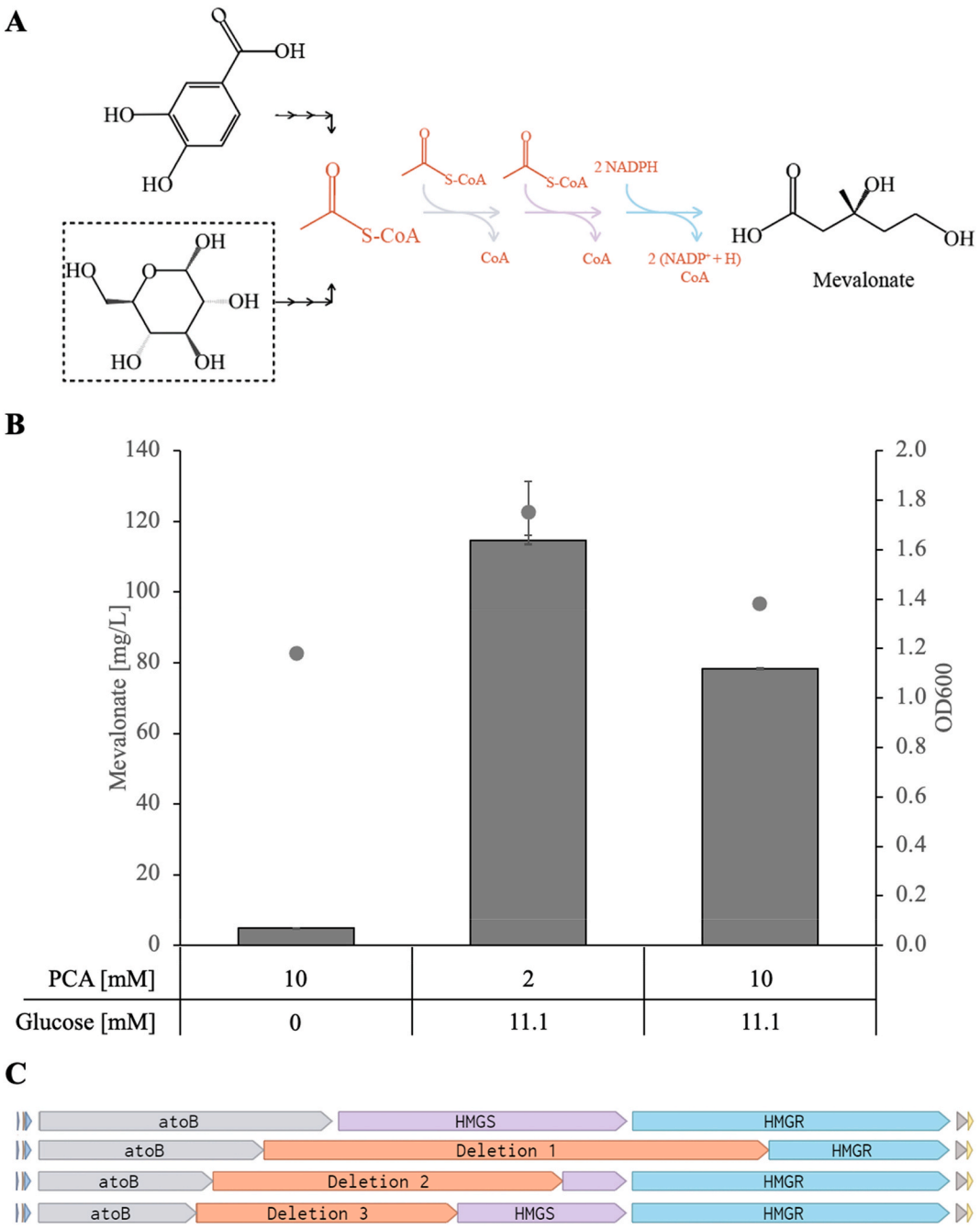

Fig. 1. ADP1 produces mevalonate, but plasmid instability reduces production in PCA-only condition. ADP1 was cultured in batch mode for 24 hours with expression of the mevalonate pathway. (A) The mevalonate pathway comprising *atoB, ERG13,* and *HMG1*, catalyzes the conversion of three molecules of acetyl-CoA into mevalonate. (B) Mevalonate was detected in all conditions, including in medium containing solely 10 mM PCA ($p = 0.01$, *t*-test, 2-tailed). The primary vertical axis shows mevalonate production. The secondary vertical axis shows OD_{600}. Data is mean and error bars represent S.E.M. ($n = 2$). (C) Plasmid instability in the 10 mM PCA condition occurred for glucose-free medium. The top band represents the full pathway, with the second, third, and fourth bands being distinct mutants found in the 10 mM PCA-only condition cultures.

mevalonate pathway present in PCA-only cultures [Fig. 1 C]. These deletions occurred at various loci and impacted multiple genes in the mevalonate pathway. PCA is known as a poor substrate due to its tendency to chelate iron, which may have caused significant cellular stress (Garner et al., 2004). Glucose appears to obviate this stress and stabilize the plasmid.

3.2. *Mevalonate production is affected by the aromatic acid species present*

After seeing mevalonate titers were very sensitive to carbon source, we examined the productivity in the presence of various lignin-derived aromatic acids (Salvachúa et al., 2015). Aromatic acid substrates were chosen to represent both branches of the β-ketoadipate pathway, funneling either to PCA (POB and ferulate) or catechol (benzoate and anthranilate) (Salvachúa et al., 2015). To reduce growth-inhibition effects, ferulate, benzoate, and anthranilate were supplied at 5 mM

concentration, while POB was supplied at 20 mM concentration (Fischer et al., 2008) [Suppl. Fig. 2]. All culture medium contained either POB, ferulate, benzoate, or anthranilate and 0.18% (w/v) (10 mM) glucose as a supplemental carbon source. The glucose was added to ensure plasmid stability. At 48 hours, cultures were harvested and analyzed for mevalonate production [Fig. 2]. Ferulate/glucose cultures resulted in the lowest average titer of mevalonate, which may be due to lower tolerance of ferulate by ADP1 relative to other monomers (Luo et al., 2019). Cultures grown with POB/glucose had 4.6-fold higher titer relative to the other carbon source cultures tested [Fig. 2A]. To interrogate whether this was an artifact of the abundance of POB relative to other carbon sources, the carbon utilization, as c-mmoles of mevalonate per c-mole of substrate (for both POB and glucose), was calculated. Analysis of carbon utilization revealed a statistically significant increase in carbon yield for POB cultures over ferulate, benzoate, and anthranilate [Fig. 2B]. Due to its higher production per OD and low toxicity, POB/glucose was chosen as the carbon source mixture for future cultivations.

3.3. Mevalonate is efficiently produced from p-hydroxybenzoate as sole carbon source

Because POB performed well when glucose was supplemented, we conducted batch cultivation of ADP1 pMev-LacI-trc (ECA10) with M9 minimal medium containing 20 mM POB as the sole carbon source and observed increased mevalonate production relative to the PCA-containing cultures [Suppl. Fig. 1]. For cultures containing solely 20 mM POB, solely 10 mM glucose, or a mixture of 20 mM POB and 10 mM glucose as carbon sources, no mutations to the mevalonate plasmid were observed. Mixed carbon substrates led to the highest titers and are more representative of the native growth conditions of ADP1 (Linger et al., 2014). Accordingly, glucose was included as a secondary carbon source in subsequent experiments.

3.4. Removing wax ester synthesis and culturing in fed-batch enables higher production of mevalonate from aromatic carbon

Next, we studied the impact of competition for acetyl-CoA on mevalonate production. The wax ester pathway competes for acetyl-CoA through fatty acid synthesis and is known to be highly active in ADP1 under carbon-rich and nutrient-limited, particularly nitrogen-limited,

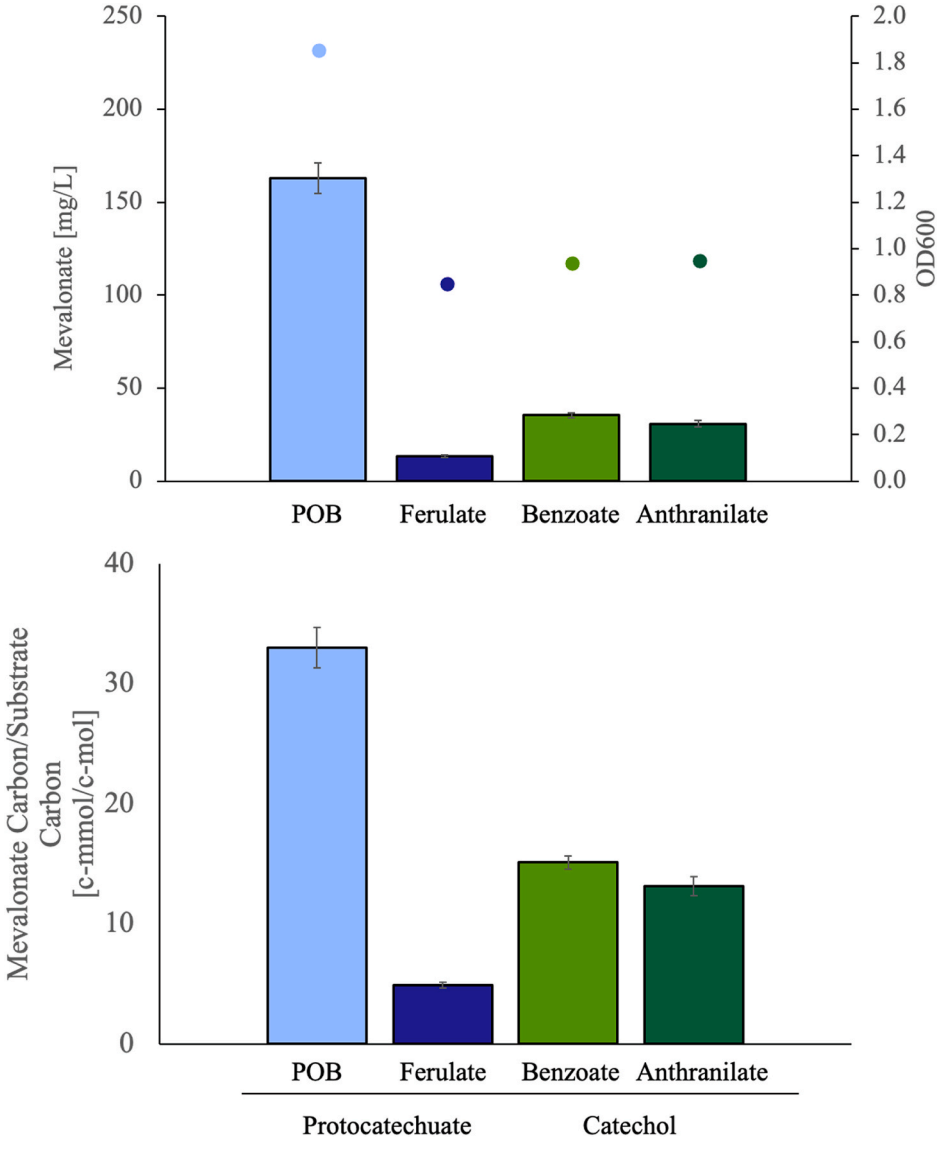

Fig. 2. Aromatic substrates affect growth, titer, and yield. As PCA only condition resulted in low titers and mutations, we screened four aromatics to determine which was best tolerated. Glucose was included to repress mutations found in aromatic only experiments. (A) Mevalonate titers (left axis) and optical density (right axis) after 48 h. (B) Carbon-molar yield of mevalonate on substrate. Both glucose and aromatic carbon were included as substrate. Data reflect mean, and error bars are S.E.M. (n = 4).

conditions (Alvarez and Steinbüchel, 2002). Fed-batch cultivation was utilized to enable conditions that were carbon-rich and nutrient-limited.

ADP1Δ*acr1* pMev-LacI-trc (ECA15) was evaluated alongside ADP1 pMev-LacI-trc (ECA10) for long-term mevalonate production in 168 hour fed-batch cultivations [Fig. 3A]. Three conditions were evaluated for mevalonate production – one with addition of POB boli, one with glucose boli, and a non-fed culture with no additional carbon subsequently added. The data show a significant 7.5-fold increase in mevalonate production in the wax ester knock-out strain compared to WT in the POB fed-batch. For the wax ester knock-out strain expressing the mevalonate pathway, cultures reached a titer of 1014 ± 379 mg/L (6.8 mM ± 2.6 mM) with a yield of 41.4 ± 17.6 c-mmol/c-mol of all substrate consumed at 168 h. Glucose fed-batch also compared favorably in the wax ester knock-out compared to WT, although to a lesser extent than POB. Cultures not supplied with additional non-carbon nutrients exhibited slow or insignificant growth rate after initial exponential phase growth [Suppl. Fig. 3].

A time-course analysis of mevalonate concentration revealed that mevalonate production continued via POB catabolism even after the initial glucose was depleted [Fig. 3B, Suppl. Fig. 4 A and D]. No other C_6 compound was detected by HPLC. These data indicate that mevalonate was being produced directly from lignin-derived carbon sources over an extended timeframe. Active synthesis of mevalonate after early stationary phase and improved mevalonate synthesis in the wax ester knockout strain supports the hypothesis that the wax ester pathway competes with the mevalonate pathway for acetyl-CoA flux under

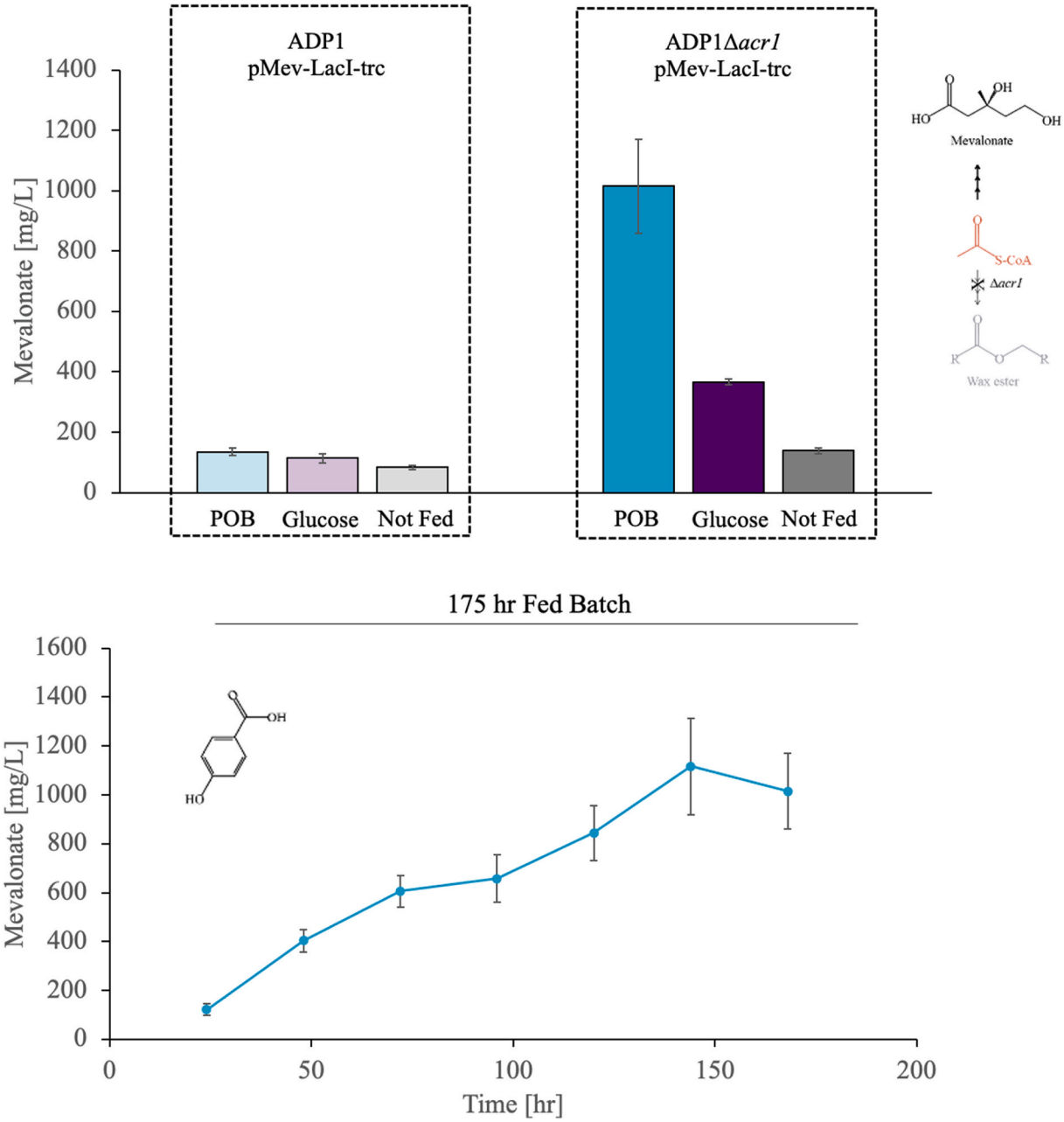

Fig. 3. Mevalonate production is improved by wax ester knock-out and fed-batch cultivation. *A. baylyi* ADP1 pMev-LacI-trc (ECA10) and the wax ester knock-out, ADP1Δ*acr1* pMev-LacI-trc (ECA15) were cultivated in fed-batch. Cultures initially contained 20 mM POB and 10 mM glucose. Cultures were fed every 24 hours one bolus of 20 mM substrate, either *p*-hydroxybenzoate (POB) or glucose, or not fed, as indicated. (A) Mevalonate titers after 168 h of POB fed-batch. (B) Mevalonate titers over culture time for in ADP1Δ*acr1* pMev-LacI-trc (ECA15) with POB feeding. Data reflect mean and error bars represent S.E.M. (n = 6 for ADP1 pMev-LacI-trc POB, glucose, not fed, and for ADP1Δ*acr1* pMev-LacI-trc POB, and n = 2 for ADP1Δ*acr1* pMev-LacI-trc glucose and not fed).

carbon-rich, nutrient depleted conditions (Alvarez and Steinbüchel, 2002; Salmela et al., 2019). Amplification of the mevalonate pathway in the 168-h cell pellets revealed truncation of the mevalonate pathway for four of twelve POB-fed cultures and for six of eight glucose-fed cultures [Suppl. Table 4; Suppl. Fig. 5]. This is consistent with the large spread in mevalonate titers late in the POB culture [Fig. 3B]. Glucose-fed cultures exhibited significant accumulation of glucose-derived gluconate that contributed to decreased pH [Suppl. Table 5] and may have led to mutations to the mevalonate pathway, both of which may have reduced or eliminated mevalonate production [Suppl. Fig. 4 B and E; Suppl. Fig. 5]. Therefore, we postulate that mutations are likely driven by poor cell fitness due to non-optimal pH or high substrate accumulation [Suppl. Fig. 4 B and E; Suppl. Fig. 5]. Taken together, these data indicate that mevalonate production was significantly improved by eliminating the wax ester pathway and that implementing fed-batch cultivation led to continued production of mevalonate from POB after glucose was depleted, although long-term stability remains a challenge.

4. Conclusions

By utilizing the diverse metabolism and genetic maleability of ADP1, we engineered a strain capable of producing titers of mevalonate up to 1014 mg/L (6.8 mM) from mixed glucose and lignin-derived aromatic carbon sources. The strain showed functional expression of a heterologous pathway in the presence of multiple lignin-derived aromatic compounds, and production capability was significantly improved by a genetic knock-out targeting wax ester synthesis. In the future, our work will address the long-term stability of the mevalonate pathway. Genetic instability that gradually eliminates mevalonate production poses an obstacle to industrial applications of this strain. Chromosomal integration may enable expression while limiting plasmid-based metabolic burden, but it is unlikely to completely alleviate pathway burden. Based on our data, culture medium containing a mixture of aromatic and sugar-based carbon sources may reduce mutational frequency, indicating promise for future lignin-based medium optimization. In all, this work lays a foundation for lignin-based metabolic engineering to produce mevalonate pathway products in *Acinetobacter baylyi* ADP1 and provides a case study for exploring the impact of the expression of a burdensome heterologous pathway on native ADP1 metabolism.

Credit author statement

Erika Arvay: Conceptualization; Methodology; Formal Analysis; Investigation; Writing – Original Draft; Visualization; Bradley W. Biggs: Conceptualization; Investigation; Methodology; Resources; Writing – Review and Editing; Laura Guerrero: Validation; Investigation; Writing – Review and Editing; Virginia Jiang: Validation; Investigation; Writing – Review and Editing; Keith EJ Tyo: Conceptualization; Methodology; Resources; Writing – Review and Editing; Supervision; Funding Acquisition.

Funding

This work was supported by the National Science Foundation [MCB-1614953, REU DBI- 1757973] and the Northwestern Biotechnology Training Program through the National Institutes of Health [T32 GM008449].

CRediT authorship contribution statement

Erika Arvay: Conceptualization, Methodology, Formal analysis, Investigation, Writing – original draft, Visualization. **Bradley W. Biggs:** Conceptualization, Investigation, Methodology, Resources, Writing – review & editing. **Laura Guerrero:** Validation, Investigation, Writing – review & editing. **Virginia Jiang:** Validation, Investigation, Writing – review & editing. **Keith Tyo:** Conceptualization, Methodology, Resources, Writing – review & editing, Supervision, Funding acquisition.

Acknowledgements

We would like to thank Prof. Ellen Neidle for providing materials, Dr. Gregg Beckham for helpful discussions, and Dr. Namita Bhan for helpful discussions and proofreading. We would like to acknowledge the NUSeq Core Facility for sample analysis and the Integrated Molecular Structure Education and Research Center (IMSERC) at Northwestern University for technical assistance.

Appendix A. Supplementary data

Supplementary data to this article can be found online at https://doi.org/10.1016/j.mec.2021.e00173.

References

Ajikumar, P.K., Tyo, K., Carlsen, S., Mucha, O., Phon, T.H., Stephanopoulos, G., 2008. Terpenoids: opportunities for biosynthesis of natural product drugs using engineered microorganisms. Mol. Pharm. 5 (2), 167–190. https://doi.org/10.1021/mp700151b.

Alonso-Gutierrez, J., Chan, R., Batth, T.S., Adams, P.D., Keasling, J.D., Petzold, C.J., Lee, T.S., 2013. Metabolic engineering of Escherichia coli for limonene and perillyl alcohol production. Metab. Eng. 19, 33–41. https://doi.org/10.1016/j.ymben.2013.05.004.

Alvarez, H.M., Steinbüchel, A., 2002. Triacylglycerols in prokaryotic microorganisms. Appl. Microbiol. Biotechnol. 60 (4), 367–376. https://doi.org/10.1007/s00253-002-1135-0.

Bryksin, Anton V., Matsumura, Ichiro, 2010. Overlap extension PCR cloning: a simple and reliable way to create recombinant plasmids. Biotechniques 48 (6), 463–465. https://doi.org/10.2144/000113418.

Barbe, V., Vallenet, D., Fonknechten, N., Kreimeyer, A., Oztas, S., Labarre, L., Cruveiller, S., Robert, C., Duprat, S., Wincker, P., Ornston, L.N., Weissenbach, J., Marlière, P., Cohen, G.N., Médigue, C., 2004. Unique features revealed by the genome sequence of Acinetobacter sp. ADP1, a versatile and naturally transformation competent bacterium. Nucleic Acids Res. 32 (19), 5766–5779. https://doi.org/10.1093/nar/gkh910.

Beckham, G.T., Johnson, C.W., Karp, E.M., Salvachúa, D., Vardon, D.R., 2016. Opportunities and challenges in biological lignin valorization. Curr. Opin. Biotechnol. 42 (March), 40–53. https://doi.org/10.1016/j.copbio.2016.02.030.

Belcher, M.S., Mahinthakumar, J., Keasling, J.D., 2020. New frontiers: harnessing pivotal advances in microbial engineering for the biosynthesis of plant-derived terpenoids. Curr. Opin. Biotechnol. 65, 88–93. https://doi.org/10.1016/j.copbio.2020.02.001.

Biggs, B.W., Bedore, S.R., Arvay, E., Huang, S., Subramanian, H., Mcintyre, E.A., Duscent-maitland, C.V., Neidle, L., Tyo, K.E.J., 2020. Development of a genetic toolset for the highly engineerable and metabolically versatile Acinetobacter baylyi ADP1. Nucleic Acids Res. 1–14. https://doi.org/10.1093/nar/gkaa167.

Blomfield, I.C., Vaughn, V., Rest, R.F., Eisenstein, B.I., 1991. Allelic exchange in Escherichia coli using the Bacillus subtilis sacB gene and a temperature-sensitive pSC101 replicon. Mol. Microbiol. 5 (6), 1447–1457.

Bryksin, A.V., Matsumura, I., 2010. Rational design of a plasmid origin that replicates efficiently in both gram-positive and gram-negative bacteria. PloS One 5 (10). https://doi.org/10.1371/journal.pone.0013244.

Dueber, J.E., Wu, G.C., Malmirchegini, G.R., Moon, T.S., Petzold, C.J., Ullal, A.V., Prather, K.L.J., Keasling, J.D., 2009. Synthetic protein scaffolds provide modular control over metabolic flux. Nat. Biotechnol. 27 (8), 753–759. https://doi.org/10.1038/nbt.1557.

Elliott, K.T., Neidle, E.L., 2011. Acinetobacter baylyi ADP1: transforming the choice of model organism. IUBMB Life 63 (12), 1075–1080. https://doi.org/10.1002/iub.530.

Fischer, R., Bleichrodt, F.S., Gerischer, U.C., 2008. Aromatic degradative pathways in Acinetobacter baylyi underlie carbon catabolite repression. Microbiology 154 (10), 3095–3103. https://doi.org/10.1099/mic.0.2008/016907-0.

Garner, B.L., Arceneaux, J.E.L., Byers, B.R., 2004. Temperature control of a 3,4-dihydroxybenzoate (protocatechuate)-based siderophore in Bacillus anthracis. Curr. Microbiol. 49 (2), 89–94. https://doi.org/10.1007/s00284-004-4286-7.

Gibson, D.G., Young, L., Chuang, R.Y., Venter, J.C., Hutchison, C.A., Smith, H.O., 2009. Enzymatic assembly of DNA molecules up to several hundred kilobases. Nat. Methods 6 (5), 343–345. https://doi.org/10.1038/nmeth.1318.

Ishige, T., Tani, A., Takabe, K., Kawasaki, K., Sakai, Y., Kato, N., 2002. Wax ester production from n-alkanes by acinetobacter sp. strain M-1: ultrastructure of cellular inclusions and role of acyl coenzyme A reductase. Appl. Environ. Microbiol. 68 (3), 1192–1195. https://doi.org/10.1128/AEM.68.3.1192.

Juni, E., Janik, A., 1969. Transformation of acinetobacter calco-aceticus (bacterium anitratum). J. Bacteriol. 98 (1), 281–288.

Linger, J.G., Vardon, D.R., Guarnieri, M.T., Karp, E.M., Hunsinger, G.B., Franden, M.A., Johnson, C.W., Chupka, G., Strathmann, T.J., Pienkos, P.T., Beckham, G.T., 2014. Lignin valorization through integrated biological funneling and chemical catalysis. Proc. Natl. Acad. Sci. U. S. A 111 (33), 12013–12018. https://doi.org/10.1073/pnas.1410657111.

Luo, J., Efimova, E., Losoi, P., Santala, V., Santala, S., 2019. Wax Ester Production in Nitrogen-rich Conditions by Metabolically Engineered Acinetobacter baylyi ADP1, p. 735274. https://doi.org/10.1101/735274. BioRxiv.

MacEachran, D.P., Sinskey, A.J., 2013. The Rhodococcus opacus TadD protein mediates triacylglycerol metabolism by regulating intracellular NAD(P)H pools. Microb. Cell Factories 12 (1), 1–12. https://doi.org/10.1186/1475-2859-12-104.

Metzgar, D., Bacher, J.M., Pezo, V., Reader, J., Döring, V., Schimmel, P., Marlière, P., de Crécy-Lagard, V., 2004. Acinetobacter sp. ADP1: an ideal model organism for genetic analysis and genome engineering. Nucleic Acids Res. 32 (19), 5780–5790. https://doi.org/10.1093/nar/gkh881.

Norgren, M., Edlund, H., 2014. Lignin: recent advances and emerging applications. Curr. Opin. Colloid Interface Sci. 19 (5), 409–416. https://doi.org/10.1016/j.cocis.2014.08.004.

Ragauskas, A.J., Beckham, G.T., Biddy, M.J., Chandra, R., Chen, F., Davis, M.F., Davison, B.H., Dixon, R.A., Gilna, P., Keller, M., Langan, P., Naskar, A.K., Saddler, J. N., Tschaplinski, T.J., Tuskan, G.A., Wyman, C.E., 2014. Lignin valorization: improving lignin processing in the biorefinery. Science 344 (6185). https://doi.org/10.1126/science.1246843.

Salmela, M., Lehtinen, T., Efimova, E., Santala, S., Santala, V., 2019. Alkane and wax ester production from lignin-related aromatic compounds. Biotechnol. Bioeng. 116 (8), 1934–1945. https://doi.org/10.1002/bit.27005.

Salvachúa, D., Karp, E.M., Nimlos, C.T., Vardon, D.R., Beckham, G.T., 2015. Towards lignin consolidated bioprocessing: simultaneous lignin depolymerization and product generation by bacteria. Green Chem. 17 (11), 4951–4967. https://doi.org/10.1039/c5gc01165e.

Santala, S., Efimova, E., Kivinen, V., Larjo, A., Aho, T., Karp, M., Santala, V., 2011. Improved triacylglycerol production in Acinetobacter baylyi ADP1 by metabolic engineering. Microb. Cell Factories 10 (1), 36. https://doi.org/10.1186/1475-2859-10-36.

Santala, S., Efimova, E., Koskinen, P., Karp, M.T., Santala, V., 2014. Rewiring the wax ester production pathway of acinetobacter baylyi ADP1. ACS Synth. Biol. 3 (3), 145–151. https://doi.org/10.1021/sb4000788.

Schutyser, W., Renders, T., Van Den Bosch, S., Koelewijn, S.F., Beckham, G.T., Sels, B.F., 2018. Chemicals from lignin: an interplay of lignocellulose fractionation, depolymerisation, and upgrading. Chem. Soc. Rev. 47 (3), 852–908. https://doi.org/10.1039/c7cs00566k.

Suárez, G.A., Dugan, K.R., Renda, B.A., Leonard, S.P., Gangavarapu, L.S., Barrick, J.E., 2019. Rapid and assured genetic engineering methods applied to Acinetobacter baylyi ADP1 genome streamlining. https://doi.org/10.1101/754242.

Vaneechoutte, M., Young, D.M., Ornston, L.N., Baere, T. De, Nemec, A., Reijden, T. Van Der, Carr, E., Tjernberg, I., Dijkshoorn, L., 2006. Naturally transformable acinetobacter sp. strain ADP1 belongs to the newly described species acinetobacter baylyi. Appl. Environ. Microbiol. 72 (1), 932–936. https://doi.org/10.1128/AEM.72.1.932.

Wang, J., 2017. Engineering of a highly efficient Escherichia coli strain for mevalonate fermentation through chromosomal integration. Appl. Environ. Microbiol. 2 (24), 1069–1079. https://doi.org/10.1128/AEM.02178-16.

Zhang, Y., Nielsen, J., Liu, Z., 2017. Engineering yeast metabolism for production of terpenoids for use as perfume ingredients, pharmaceuticals and biofuels. FEMS Yeast Res. 17 (8), 1–11. https://doi.org/10.1093/femsyr/fox080.